Provided for non-commercial research and education use.
Not for reproduction, distribution or commercial use.

This article appeared in a journal published by Elsevier. The attached copy is furnished to the author for internal non-commercial research and education use, including for instruction at the authors institution and sharing with colleagues.

Other uses, including reproduction and distribution, or selling or licensing copies, or posting to personal, institutional or third party websites are prohibited.

In most cases authors are permitted to post their version of the article (e.g. in Word or Tex form) to their personal website or institutional repository. Authors requiring further information regarding Elsevier's archiving and manuscript policies are encouraged to visit:

http://www.elsevier.com/copyright

Author's personal copy

Ultrasonics Sonochemistry 18 (2011) 1165–1171

Contents lists available at ScienceDirect

Ultrasonics Sonochemistry

journal homepage: www.elsevier.com/locate/ultsonch

Effect of local dual frequency sonication on drug distribution from polymeric nanomicelles

Hadi Hasanzadeh [a,1], Manijhe Mokhtari-Dizaji [a,*], S. Zahra Bathaie [b], Zuhair M. Hassan [c]

[a] Department of Medical Physics, Faculty of Medical Sciences, Tarbiat Modares University, Tehran, Iran
[b] Department of Clinical Biochemistry, Faculty of Medical Sciences, Tarbiat Modares University, Tehran, Iran
[c] Department of Immunology, Faculty of Medical Sciences, Tarbiat Modares University, Tehran, Iran

ARTICLE INFO

Article history:
Received 17 January 2011
Received in revised form 12 March 2011
Accepted 17 March 2011
Available online 1 April 2011

Keywords:
Ultrasound
Acoustic cavitation
Nanotechnology
Drug delivery
Breast adenocarcinoma

ABSTRACT

To overcome the side effects caused by systemic administration of doxorubicin, nanosized polymeric micelles were used in combination with dual frequency ultrasonic irradiation. These micelles release the drug due to acoustic cavitation, which is enhanced in dual frequency ultrasonic fields. To form the drug-loaded micelles, Pluronic P-105 copolymer was used, and doxorubicin was physically loaded into stabilized micelles with an average size of 14 nm. In this study, adult female Balb/C mice were transplanted with spontaneous breast adenocarcinoma tumors and were injected with a dose of 1.3 mg/kg doxorubicin in one of three forms: free doxorubicin, micellar doxorubicin without sonication and micellar doxorubicin with sonication. To increase cavitation yield, the tumor region was sonicated for 2.5 min at simultaneous frequencies of 3 MHz (I_{SATA} = 2 W/cm^2) and 28 kHz (I_{SATA} = 0.04 W/cm^2). The animals were sacrificed 24 h after injection, and their tumor, heart, spleen, liver, kidneys and plasma were separated and homogenized. The drug content in the tissues was determined using tissue fluorimetry (350 nm excitation and 560 nm emission), and standard drug dose curves were obtained for each tissue. The results show that in the group that received micellar doxorubicin with sonication, the drug concentration in the tumor tissue was significantly higher than in the free doxorubicin injection group (8.69 times) and the micellar doxorubicin without sonication group (2.60 times). The drug concentration in other tissues was significantly lower in the micellar doxorubicin with sonication group relative to the free doxorubicin (3.35 times) and the micellar drug without sonication (2.48 times) groups ($p < 0.05$). We conclude that dual frequency sonication improves drug release from micelles and increases the drug uptake by tumors due to sonoporation. The proposed drug delivery system creates an improved treatment capability while reducing systemic side effects caused by drug uptake in other tissues.

© 2011 Elsevier B.V. All rights reserved.

1. Introduction

The main mechanisms of biological action for ultrasound include the generation of thermal energy, sonoporation, the enhancement of local microjets due to inertial cavitation (which are further enhanced by multifrequency sonication [1–3] and the enhanced permeability of blood capillaries [4–10]. All of these mechanisms could potentially be used to enhance drug uptake locally. Doxorubicin is of great importance in the treatment of leukemia and solid tumors such as in breast and ovarian cancer and sarcoma pulmonary metastasis, but its clinical use is hampered by its myelotoxicity and its cumulative cardiotoxicity when administered systemically [11–15]. By targeting this drug to the desired site of action and increasing its uptake using sonication, the side effects are minimized and the therapeutic efficiency is increased. Various nanosized carriers such as liposomes [16], polymeric micelles [17,18] and core–shell nanoparticles [15,19–21] have been reported as vehicles for passive targeting. Polymeric micelles [22] and core–shell nanoparticles [19,23] have received considerable attention due to their self-assembly characteristics in an aqueous solution. These properties offer the possibility for a unique biodistribution of drugs to target solid tumors [18], and it has been reported that doxorubicin-conjugated block copolymer micelles were effective in the treatment of solid tumors due to prolonged circulation in the blood [17,24]. Generally, it has been reported that anticancer agents incorporated in polymeric micelles have an enhanced blood circulation time (EPR: enhanced penetration and retention effect) and a suppressive effect on the growth of solid tumors [18,21–24]. Many polymeric micelles are convenient to use because they can conveniently escape the reticuloendothelial system (RES) and undergo renal extraction because of their

* Corresponding author. Tel.: +98 21 82883893; fax: +98 21 88006544.
E-mail address: mokhtarm@modares.ac.ir (M. Mokhtari-Dizaji).
[1] Present address: Assistant Professor in Medical Physics, Department of Medical Physics, Semnan University of Medical Sciences, Semnan, Iran.

1350-4177/$ - see front matter © 2011 Elsevier B.V. All rights reserved.
doi:10.1016/j.ultsonch.2011.03.018

Author's personal copy

small size, which is approximately 20–100 nm [24–27]. Various methods to quantify doxorubicin in biological fluids have been reviewed [28]. Reversed-phase liquid chromatography coupled with fluorescence detection is the method of choice to assay of doxorubicin [29–31], although alternative schemes such as electrochemical detection [32], UV spectrophotometric [33] detection and mass spectrometry [34] have also been used. However, fluorescence detection is often the most appropriate detection method for doxorubicin considering its simplicity of use, selectivity and sensitivity [11].

In this study, polymeric micelles were prepared using Pluronic P-105, which is a triblock copolymer consisting of blocks of PPO (Poly Propylene Oxide) and PEO (Poly Ethylene Oxide) in the form PEO_{37}–PPO_{56}–PEO_{37}. After loading doxorubicin into these micelles and checking the drug release upon sonication *in vitro*, their anti-tumor effect was tested *in vivo*. Ultrasound was used to enhance the intracellular drug uptake from micelles. Using a spectrophotometric method, the drug content in several tissues was quantified.

2. Materials and methods

2.1. Animal model

Female inbred Balb/C (6–8 weeks) mice were purchased from the breeding colony at the Pasteur Institute of Iran (Tehran, Iran). Mice were housed under standard conditions (constant temperature, humidity and 12 h dark–light cycles) and had access to food and water ad libitum. The tumor model was a syngenic of murine spontaneous breast adenocarcinoma, which was chopped into fresh pieces of about 2–3 mm diameter and then transplanted into the flank region of the mice. Tumors reached a diameter of about 7–9 mm in 7–10 days, at which point they were ready to be used in experiments. All animal experiments and protocols were evaluated and approved by the Animal and Ethics Review Committee of the Tarbiat Modares University (Tehran, Iran).

2.2. Ultrasonic setup and sonication conditions

Two ultrasonic systems were used in a cubic Perspex water tank ($25 \times 20 \times 20\ cm^3$) in an orthogonal geometry. The first system was designed in our lab (Tarbiat Modares University, Ultrasound Lab, Tehran, Iran) in collaboration with the Pars Nahand Engineering company (Pardis Technology Park, Tehran, Iran) to operate in the low kHz range with a center frequency of 27.7 kHz (nominal frequency of 28 kHz), a bandwidth of 421 Hz and a probe diameter of 60 mm. The second system was a 3-MHz therapeutic unit (SM3670, Shrewsbury Medical Ltd., Shropshire, UK) with a 30-mm-diameter probe and 5-cm^2 effective radiation area (ERA). Probes were held fixed in the tank wall through a pair of circular holes in such a way that the central beam axis for each probe was perpendicular to the other. Acoustic calibration for the power and intensity of the devices was carried out in degassed water in the tank using a radiation force balance (Shrewsbury Medical Co., Shropshire, UK, ±10%) for the therapeutic unit and the hydrophone method in the cubic chamber for our unit (PA124, Precision Acoustics Ltd., Dorchester, Dorset, UK; calibration range: 10 kHz–3 MHz with a sensor diameter of 25 mm). Different single frequency sonication conditions including 28 kHz (0.02 and 0.04 W/cm^2) and 3 MHz (1 and 2 W/cm^2) were demonstrated (Hasanzadeh et al., 2010). In addition, a dual frequency combination (28 kHz + 3 MHz) at the above-mentioned intensities was studied. All reported experimental intensity values consist of the spatial average/temporal average (I_{SATA}). In each sonication condition, subharmonic signal amplitudes at 14 kHz and 1.5 MHz in the water tank were recorded with the hydrophone. All of the above conditions were applied in a continuous wave mode and for a sonication duration of 3 min. Each recorded signal comprised of 32768 data points collected with a sampling rate of 10 MHz, which includes the primary frequency and the pressure waves coming from the oscillating walls of the cavities. To extract the frequency contents, signals were analyzed in MATLAB software version 7.0.1 (Mathworks, USA) using an FFT function with a hamming window. Background noise was measured by placing the hydrophone in the usual measurement conditions and setting the intensity of the unit to zero; this background was subtracted from the signal amplitude in each measurement condition. The subharmonic peak in the FFT of the measured pressure signal was recorded. Each experimental condition was repeated 5 times.

2.3. Chemicals

Doxorubicin was obtained from Pharmacia (Italy). Pluronic P-105 was provided by the BASF Corp. (Mount Olive, NJ, USA). N-N-Diethylacrylamide (NNDEA) was obtained from Polysciences (Warrington, USA). N,N′-Bis(acryloyl)cystamine (BAC) was obtained from Fluka (Sigma–Aldrich, UK), and benzoyl peroxide (BP) was obtained from Merck (Merck KGaA, Darmstadt, Germany).

2.4. Preparation of micelles

Polymeric micelles were prepared using Pluronic P-105, which is a triblock copolymer consisting of blocks of poly (propylene oxide) (PPO) and poly (ethylene oxide) (PEO) in the form PEO_{37}–PPO_{56}–PEO_{37}. A solution of NaCl and 10 wt.% Pluronic P-105 in distilled water was added to a round-bottom balloon, which was stirred for 20 min while immersed in a water bath under a nitrogen purge at a temperature of 65 °C. A mixture of BAC, BP and NNDEA (26:1:55 weight ratio) was added to the above solution, and it was allowed to stir at this temperature under a nitrogen purge for 3.5 h. After turning the nitrogen off, the mixture was allowed to polymerize for 19.5 h. The size distribution of the micelles was measured by dynamic light scattering (DLS) (Malvern Instruments Ltd., Malvern, UK).

2.5. Loading doxorubicin into micelles

To load doxorubicin into injectable micelles, it was necessary to find the optimal drug loading into micelles through a standard curve, which was measured using a UV spectrophotometer (Shimadzu, Model RF-1500, Japan) at 350 nm.

To obtain the curve, several known concentrations (0–0.12 mg of doxorubicin in a 1 ml solution of micelles) were prepared, and their fluorescence emissions were read at 350 nm. It is notable that at higher concentrations, the fluorescent emission decreases due to self-quenching of the doxorubicin. Fluorescence intensity (counts) versus doxorubicin concentration (mg/ml) yielded a straight line of positive slope for increasing concentrations. The results show that there is a significant correlation between the fluorescence intensity and the doxorubicin concentration ($R^2 = 0.96$, correlation is significant at 0.01). A linear regression analysis was applied between the fluorescence intensity and the doxorubicin concentration and the results are shown in Fig. 1.

To examine drug release *in vitro*, a custom exposure chamber was constructed according to the spectrophotometric characteristics of doxorubicin obtained above ($\lambda_{ex} = 350$ nm, $\lambda_{em} = 560$ nm); this chamber recorded the change in light emission due to doxorubicin release under sonication (Fig. 2). A digital camera (Sony, DSC P-93, Japan) with a multi-band filter (Alexa Fluor® 350/488/594, USA) was used to record images (BMP images with dimensions of 640×480 pixels), and a background was recorded without son-

Author's personal copy

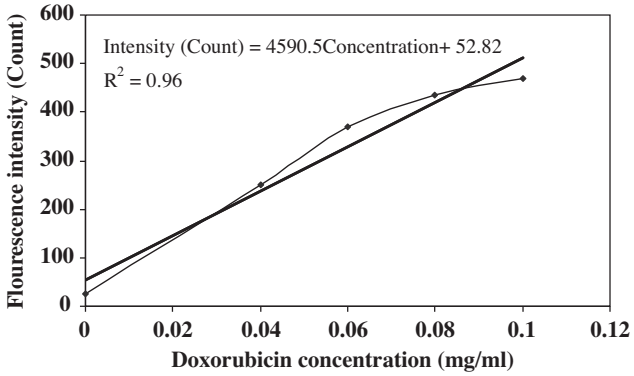

Fig. 1. Micellar drug loading standard curve.

ication. The frequency and intensity were selected previously using a subharmonic analysis method to enhance the acoustic cavitation at 28 kHz and 3 MHz [35].

Each sonication protocol was run 5 times, and the *RMSE* (root mean square error) values of the images were used to compare between images:

$$RMSE = \sqrt{\sum_{i=0}^{n} \frac{(x_i - x_i')^2}{n}} \quad (1)$$

In the above equation, x_i and x_i' are signal amplitudes of the images in each group and the background images, respectively. Finally, the average of the *RMSEs* of the image components was used to compare the ability of different sonication conditions to release the drug from the micelles.

Doxorubicin was stirred into the micellar solution to load it into the micelles; to separate the free drug from the encapsulated drug, the solution was filled into a dialysis bag (30 mm diameter, 5 kDa cut off, BioGene, Mashhad, Iran) and dialyzed against water for 2 h. The correct time was determined by sampling from the dialysis bag at different times until the drug fluorescence no longer changed. According to the standard curve of the drug in micelles, the optimum drug loading into micelles was determined. All experiments were performed in triplicate.

2.6. Stability studies of the micellar drug

To investigate the stability of the micellar drug, the fluorescence amplitude of the micellar drug at 350 nm was measured over time, and the amplitude of this emission from each day was normalized to day zero (the time of drug encapsulation) to find the stability of the complex. The complex was stored at 4 °C, and its stability was measured for one month.

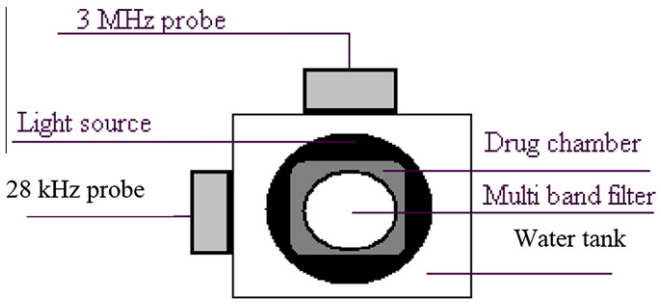

Fig. 2. Setup for the measurement of doxorubicin release *in vitro*. Elements include the 3-MHz probe, the 28-kHz probe, the filter on which the camera was mounted, the light source that is placed at the bottom and the drug chamber that was placed in the water box on the light source.

2.7. Biodistribution and in vivo study

Because the goal of the current study was to work below the level of hyperthermia, it was necessary to measure the temperature rise due to sonication *in vivo*. Three female Balb/C mice were selected and placed into the sonication condition after being anesthetized. The temperatures of the tumors and their surrounding environment were monitored every second during sonication with a portable digital thermometer containing a dual thermocouple input. The tissue temperature was monitored invasively using K-type wire thermocouples (TP-01, Lutron Electronic Enterprise Co., Taiwan, −200–1372 °C, 0.1 mm thickness, ±0.1 °C). Each of these microthermometers had two wire thermocouples placed in the animal's body. The temperature changes (°C) at different depths in mice versus duration of sonication under dual frequency sonication conditions was evaluated for different depths relative to the skin in the center of the tumor (close to the ultrasonic probes) to about 4 cm below the skin until animal posterior layer in 1 cm steps. All of the thermocouples provided inputs to the control unit, which contained a microprocessor connected to a computer via an RS-232 port. The temperatures were recorded every second (as .doc files) using thermometer software (Multilogger Thermometer CHY502A, Taiwan), which was connected to a PC, and the temperature rise under sonication conditions was recorded every 30 s for 20 min. The water temperature was controlled using a digital thermometer and an electrical heater and was fixed at 32 °C. According to our temperature measurements, a 2.5 min sonication time was deemed suitable for the next phase of our *in vivo* study. We have evaluated a control group without sonication but we did not have any temperature changes. Therefore, that obtained results are due to sonication rather than a vasculature lesion provoked by probe insert in tumor mass.

To study the drug distribution in animals, 9 female Balb/C mice with tumor diameters of about 7–9 mm were randomly divided into 3 groups as follows: IV injection of free doxorubicin, IV injection of micellar doxorubicin and IV injection of micellar doxorubicin with sonication under the optimum conditions mentioned above. After drug injection via the tail vein at a dose of 1.3 mg/kg (the amount of drug injected was 26 μg for each animal in different groups), animals were anesthetized and placed in a special cage in the vicinity of the probes in the ultrasonic field; in only the sonication group, the tumor region was exposed for 2.5 min to the selected sonication protocol, which was determined by the subharmonic amplitude analysis (Fig. 3).

The concentration of total doxorubicin in plasma is maximum at 2 min following injection and decreased bi-exponentially to underdetectable levels after 24 h [15,28,33]. Therefore animals were exposed 2 min following injection. Based on previous study, the distribution of doxorubicin into tumors was maximum 24 h following injection. The levels of doxorubicin in the tumors increased until 24 h [28]. Therefore, after 24 h, the animals were sacrificed, blood was collected using a heparinated syringe from the heart, and tissues (heart, liver, spleen, kidney and tumor) were dissected and lyophilized. The blood was centrifuged (1500 rpm for 10 min), and the plasma was separated and kept for later analysis. Tissue extracts were obtained according to available protocols [36]. The doxorubicin concentration in the tissues and plasma was determined by a fluorescence assay using a UV spectrophotometer (Shimadzu, Model RF-1500, Japan) at 350 nm. Standard curves for each tissue were established by adding known amounts of doxorubicin to tissue extracts of control mice to obtain various concentrations; these curves were used later to obtain the drug concentration in different tissues from the experimental groups.

Author's personal copy

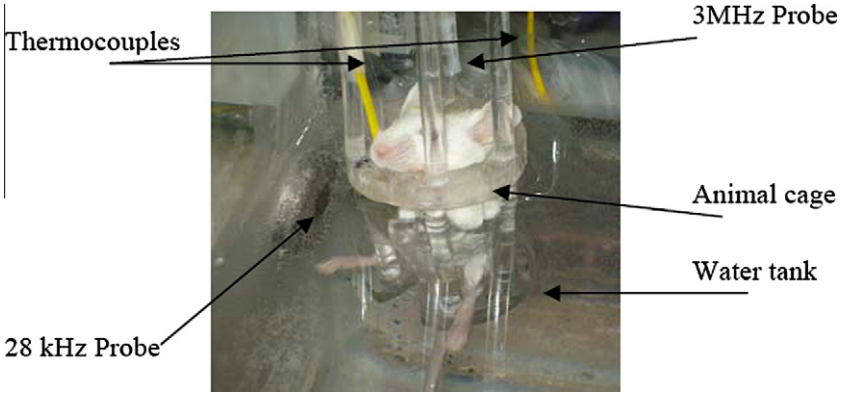

Fig. 3. Animal sonication setup. A side view of the animal cage in the sonication condition. The 28-kHz probe, 3-MHz probe and thermocouples are shown.

2.8. Statistical analysis

Statistical analysis was performed using Microsoft Excel 2003 and SPSS 16 (SPSS/PC Inc., Chicago, IL). The drug content in tissues is presented as the mean ± SD. To analyze differences between groups, a one way ANOVA was used with a level of significance of 0.05 (P-value < 0.05).

3. Results

Fig. 4 shows the results from dynamic light scattering (DSL), which gives a particle size distribution of the synthesized micelles. As shown in Fig. 4, polymeric micelles had small particle sizes with an average size of 14 nm.

The stability of the encapsulated drug was evaluated over one month. Fig. 5 shows the fluorescence amplitude of the micellar drug at 350 nm. The amplitude of this emission measurement at each day was normalized to the value from day zero. As shown in Fig. 5, the encapsulated drug is stable for the first 4 days, and about 90% of the maximum possible stability was maintained over the first ten days.

The results of a subharmonic amplitude measurement at 14 kHz during both single frequency sonication and simultaneous dual-frequency sonication at different intensities are shown in Fig. 6. For each measurement condition, the amplitude of the processed signal was extracted and recorded after the subtraction of background noise for each frequency component. One of the interesting results of this frequency combination is the synergistic effects in dual frequency sonication using 28 kHz (0.04 W/cm^2) and 3 MHz (2 W/cm^2) frequencies. The amplitude increase of dual frequency

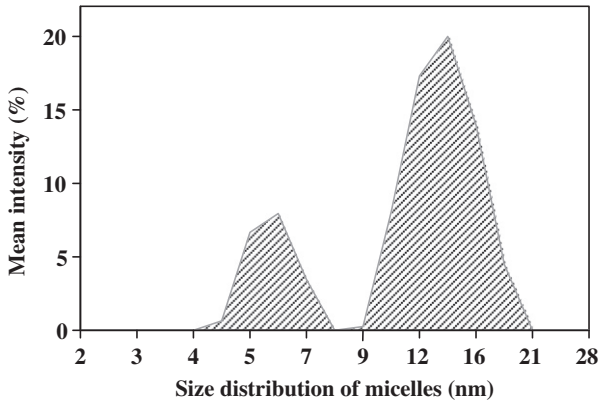

Fig. 4. Result of DLS (dynamic light scattering) on the synthesized micelles.

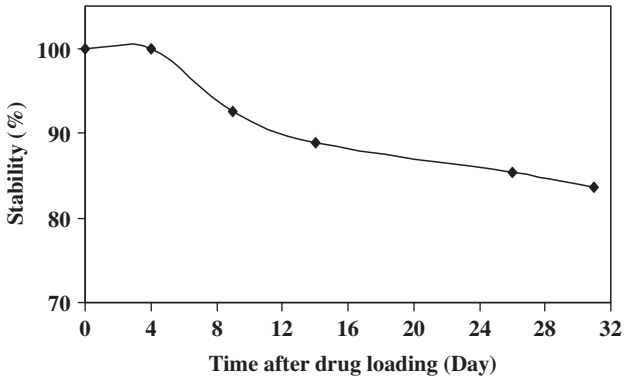

Fig. 5. Stability of the micellar drug versus time (days).

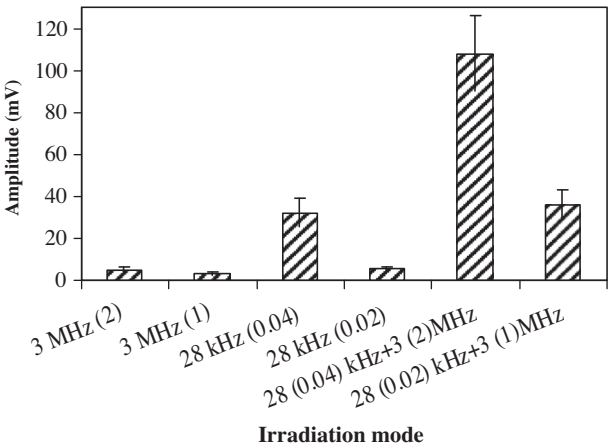

Fig. 6. Signal amplitudes (mV) at 14 kHz (a subharmonic of 28 kHz) of the 28 kHz and 3 MHz sources applied alone and in combination and presented as mean ± SD. The background has been subtracted from all values. The values in the parentheses are intensities in W/cm^2.

irradiation with respect to single frequency irradiation is due to the synergistic effect and creates an enhanced cavitation activity from the combined fields.

It has been previously shown by the authors that the 14 kHz subharmonic amplitude when applying a dual frequency combination of 28 kHz (0.04 W/cm^2) and 3 MHz (2 W/cm^2) in the continuous mode was about 5 times higher than that obtained from the algebraic sum of single 28 kHz and 3 MHz irradiation. *RMSE* values of the images from dual frequency sonication (28 kHz (0.04 W/

Author's personal copy

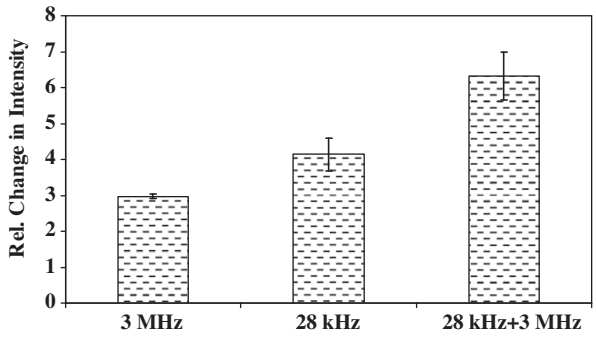

Fig. 7. RMSE values of the images (Mean ± SD) from dual frequency sonication (28 kHz (0.04 W/cm^2) and 3 MHz (2 W/cm^2)).

cm^2) and 3 MHz (2 W/cm^2)) *in vitro* are shown in Fig. 7. Drug release from the micelles is due to the cavitation activity, which is enhanced in a dual frequency field; this property is observable in the *RMSE* values.

Fig. 8 shows the temperature rise due to sonication with combined ultrasound irradiation (28 kHz (0.04 W/cm^2) + 3 MHz (2 W/cm^2)) in 30 s intervals for 20 min at several depths in the animal body. True to expectations, the temperature rise is more serious at a 1 cm depth, which is closer to the ultrasonic probes than in the other regions. The increase is also seen to some extent at the 2 cm depth, but the other two depths do not change temperature significantly. The 1 cm thermocouple was placed into tumor tissue, and the other three were placed outside the tumor. From this data, the duration of sonication in future experiments was selected to be 2.5 min; as Fig. 8 illustrates, this length of time causes a temperature rise of no more than 4 °C outside the tumor. The results indicate that a 2.5 min sonication causes a temperature rise below the level of hyperthermia ($T \leqslant 42$ °C). We have evaluated a control group without sonication but we did not have any temperature changes.

To study the drug distribution in animal tissues, three forms of doxorubicin were injected into female Balb/C mice that had tumors of about 7–9 mm diameter: free doxorubicin, micellar doxorubicin and micellar doxorubicin with sonication under optimum conditions. The doxorubicin concentration in tissues and in the plasma were determined by a fluorescence assay; the results are shown in Table 1. In this table, standard curves for each tissue were established by adding known amounts of doxorubicin to tissue extracts of control mice to obtain standard measurements at different concentrations. The results are shown and are fit with linear

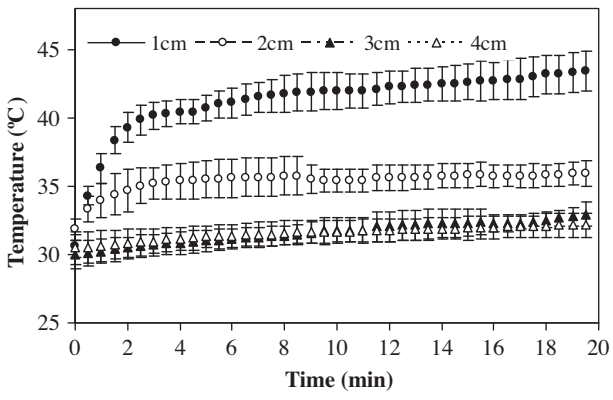

Fig. 8. The mean ± SD of temperature changes (°C) at different depths in mice (1, 2, 3 and 4 cm) versus duration of sonication (min) under dual frequency sonication conditions (3 MHz and 28 kHz).

Table 1
The standard linear regression functions for each tissue given as fluorescence intensity (X: count) versus concentration of doxorubicin (Y: μg/ml).

Tissue	Linear regression function	Correlation of coefficient	P-value
Spleen	$Y = 0.2X - 2.6$	0.98	<0.01
Heart	$Y = 0.1X - 1.6$	0.98	<0.01
Liver	$Y = 0.07X - 3.6$	0.96	<0.01
Kidney	$Y = 0.2X - 4.8$	0.98	<0.01
Tumor	$Y = 0.2X - 4.5$	0.99	<0.01
Plasma	$Y = 0.1X - 1.0$	0.99	<0.01

regression functions. Fluorescence intensity (counts) versus concentration of doxorubicin (μg/ml) for each tissue yielded a straight line of positive slope for increasing concentrations. The results show that there is a significant correlation between the fluorescence intensity and the concentration of doxorubicin ($R > 0.96$, correlation is significant at 0.01) for each tissue.

These curves were later used to obtain the drug concentration in different tissues in the studied groups. Table 2 shows the results of tissue spectrofluorimetric measurements from three different groups: free doxorubicin, micellar doxorubicin and micellar doxorubicin with 28 kHz (0.04 W/cm^2) and 3 MHz (2 W/cm^2) dual frequency sonication in continuous mode. Based on spectrofluorimetric analysis, doxorubicin content (μg) was presented as mean ± SD in different tissues.

The drug content in the group that received micellar drugs in their tumor tissue was significantly higher (3.34 times) than in the group receiving doxorubicin in its free form ($p < 0.05$). In other non-tumor tissues, the drug content in the micellar group was lower (1.35 times) than in the group that received free doxorubicin ($p < 0.05$).

4. Discussion

Ultrasound is a unique tool in the field of drug delivery because it enables improved penetration ability, which allows substances to reach deep regions in the body, and it is non-ionizing by nature. In addition, it may be used to enhance intracellular drug uptake from micelles. The biological action of ultrasound encompasses several mechanisms of action including the generation of thermal energy, sonoporation, the enhancement of local microjets due to inertial cavitation (which is enhanced in a multifrequency sonication field [1,2]) and the enhancement of the permeability of blood capillaries [4–10]. To inhibit an unwanted temperature increase in critical tissues above their tolerances, the sonication time was selected as 2.5 min. It is also expected that under multifrequency sonication conditions, enhanced cavitation activity will be observed.

The amount of drug collected from the different groups was 10.33 ± 1.02 μg for the free doxorubicin injection group, 12.64 ± 1.94 μg for the micellar doxorubicin injection group and 16.09 ± 1.07 μg for the micellar doxorubicin injection with sonication group. The amount of drug injected was 26 μg for each animal in the different groups. The difference between the amounts of collected drug and injected drug might be due to the fact that we did not collect animal urine and we used plasma instead of serum. Furthermore, to collect the drug from several tissue extracts, only the filtered supernatant of centrifuged tissue extracts was used to track the drug, but the sediments may also contain some drugs. Finally, the drug content of tissues such as the muscle, lung, gut and brain was not measured. All of these issues may cause a decrease in drug collection.

It is also apparent in Table 2 that sonication of the micellar form of the drug caused a significant increase (2.60 times) in drug uptake by the tumor and a decrease in drug uptake by other tissues (from 1.5 times for the spleen to 9.6 times for the heart). It is ex-

Author's personal copy

Table 2
Doxorubicin content (μg) presented as mean ± SD in different tissues and in different groups studied 24 h after injection.

Group	Tissue					
	Spleen	Liver	Kidney	Heart	Tumor	Plasma
Doxorubicin	2.497 ± 0.090	1.126 ± 0.093	1.901 ± 0.210	2.493 ± 0.088	1.495 ± 0.414	0.820 ± 0.121
Micellar doxorubicin	2.275 ± 0.256	0.935 ± 0.187	1.476 ± 0.574	2.306 ± 0.007	5.000 ± 0.707	0.650 ± 0.212
Micellar doxorubicin + sonication	1.499 ± 0.370	0.253 ± 0.162	0.737 ± 0.125	0.240 ± 0.125	*13.000 ± 0.285*	0.358 ± 0.030

pected that the accumulation and uptake of the drug from the micellar form in the tumor tissue will be higher (8.69 times) than the free form of the drug because of the *EPR* (Enhanced Penetration and Retention) effect. Moreover, sonication causes an increase in drug uptake because of sonoporation, which is observed in the group that was sonicated under optimum conditions.

Urva et al. studied the biological distribution of doxorubicin and showed that there is a significant decrease in drug content in the plasma in the first 30 min following injection; the spleen had the highest drug concentration relative to plasma 72 h after injection followed by the liver, kidney, lung, gut, heart, muscle, testes and brain [31]. The high uptake ability of liver tissue was observed in the study of Bibby et al., which used Balb/C mice and a metastatic mammary cell line [28]. Al-Abd et al. used doxorubicin and its polyphosphazene hydrogel mixture in their study on drug distribution. They dissected tissues 1 h after intratumoral drug injection and analyzed them for drug content; they showed that in the hydrogel mixture group, the tumor had the highest drug content, while the kidney, liver, spleen, gut, lung, heart and brain were at lower concentrations [29]. In another study on the doxorubicin profile of rat plasma, it was shown that in the first 40 min after injection, the drug content in the plasma reduces to about 1/50 its primary value [37]. In a study on nude Balb/C mice that used two different micellar forms of doxorubicin as well as free doxorubicin, it was shown that one of the micellar forms of the drug had the highest drug uptake, while the remaining groups showed maximal uptake by the liver [33]. In the present study, the group that received doxorubicin in its free form showed the highest drug content in the spleen and lower drug content in the tumor, while the group that received the micellar drug showed the highest drug concentration in the tumor. This problem can be explained by the characteristics of tumor tissues. The physiological and interstitial properties of tumors create slower lymphatic drainage than normal tissue, which causes extravasation of macromolecules to the interstitial spaces. Additionally, the lack of vascular permeability factors in tumor cells makes the tumor vasculature abnormally leaky to macromolecules, and this inability of tumor tissue to eliminate macromolecules may explain the accumulation of the polymer conjugates seen in tumors. The most notable result was the group that received the micellar drug in combination with sonication. A dual frequency sonication condition was used to reduce the cavitation area [35], and as a result, it was possible to minimize the cavitation region and control the sonoporation region *in vivo*, which causes enhanced drug uptake locally. It was observed that tumor drug uptake in this group was much more than in the group that only received the micellar drug.

It is concluded that local sonication with a dual frequency system causes the drug to release from the micellar carriers and increases drug uptake ability. We hypothesize that cavitation events caused by dual frequency sonication can disrupt micelles and release the drug into the aqueous environment.

References

[1] W. Lauterborn, T. Kurz, R. Geisler, D. Schanz, O. Lindau, Acoustic cavitation, bubble dynamics and sonoluminescence, Ultrason. Sonochem. 14 (2007) 484–491.

[2] R. Feng, Y. Zhao, C. Zhu, T.J. Mason, Enhancement of ultrasonic cavitation yield by multi-frequency sonication, Ultrason. Sonochem. 9 (2002) 231–236.

[3] A.H. Barati, M. Mokhtari-Dizaji, H. Mozdarani, S.Z. Bathaie, Z.M. Hassan, Effect of exposure parameters on cavitation induced by low-level dual-frequency ultrasound, Ultrason. Sonochem. 14 (2007) 783–789.

[4] G. Husseini, G. Myrup, W. Pitt, D. Christensen, N. Rapoport, Factors affecting acoustically triggered release of drugs from polymeric micelles, J. Contr. Release 69 (2000) 43–52.

[5] G. Husseini, D. Christensen, N. Rapoport, W. Pitt, Ultrasonic release of doxorubicin from Pluronic P105 micelles stabilized with an interpenetrating network of N,N-diethylacrylamide, J. Contr. Release 83 (2002) 303–305.

[6] G. Husseini, M.D. Rosa, T. Gabuji, Y. Zeng, D. Christensen, W. Pitt, Release of doxorubicin from unstablized and stabilized micelles under the action of ultrasound, J. Nanosci. Nanotechnol. 7 (2007) 1028–1033.

[7] A. Marine, M. Muniruzzaman, N. Rapoport, Acoustic activation of drug delivery from polymeric micelles: effect of pulsed ultrasound, J. Contr. Release 71 (2001) 239–249.

[8] Z. Gao, H. Fain, N. Rapoporrt, Controlled and targeted tumor chemotherapy by micellar encapsulated drug and ultrasound, J. Contr. Release 102 (2005) 203–222.

[9] I. Larina, B. Evers, T. Ashitkov, C. Bartels, K. Larin, R. Esenaliev, Enhancement of drug delivery in tumors by using interaction of nanoparticles with ultrasound radiation, Technol. Cancer Res. Treat. 4 (2005) 217–226.

[10] J. Nelson, B. Roeder, J. Carmen, F. Roloff, W. Pitt, Ultrasonically activated chemotherapeutic drug delivery in a rat model, Cancer Res. 62 (2002) 7280–7283.

[11] A. Kümmerle, T. Krueger, M. Dusmet, C. Vallet, Y. Pan, H.B. Ris, L.A. Decosterd, A validated assay for measuring doxorubicin in biological fluids and tissues in an isolated lung perfusion model: matrix effect and heparin interference strongly influence doxorubicin measurements, J. Pharm. Biomed. Anal. 33 (2003) 475–494.

[12] P.E. Colombo, M. Boustta, S. Poujol, F. Pinguet, P. Rouanet, F. Bressolle, M. Vert, Biodistribution of doxorubicin-alkylated poly (l-lysine citramide imide) conjugates in an experimental model of peritoneal carcinomatosis after intraperitoneal administration, Eur. J. Pharm. Sci. 31 (2007) 43–52.

[13] V. Alakhov, E. Klinski, S. Li, G. Pietrzynski, A. Venne, E. Batrakova, T. Bronitch, A. Kabanov, Block copolymer-based formulation of doxorubicin. From cell screen to clinical trials, Colloids. Surf. B. Biointerfaces 16 (1999) 113–134.

[14] A.M.M. Osman, M.M. Nemnem, A.A. Abou-Bakr, O.A. Nassier, M.T. Khayyal, Effect of methimazole treatment on doxorubicin-induced cardiotoxicity in mice, Food Chem. Toxicol. 47 (2009) 2425–2430.

[15] A. Fundar, R. Cavalli, A. Bargoni, D. Vighetto, G.P. Zara, M.R. Gasco, Non-stealth and stealth solid lipid nanoparticles (SLN) carrying doxorubicin: pharmacokinetics and tissue distribution after i.v. administration to rats, Pharmacol. Res. 42 (2000) 337–343.

[16] G.J.R. Charrois, T.M. Allen, Drug release rate influences the pharmacokinetics, biodistribution, therapeutic activity, and toxicity of pegylated liposomal doxorubicin formulations in murine breast cancer, Biochim. Biophys. Acta 1663 (2004) 167–177.

[17] M. Yokoyama, M. Miyauchi, N. Yamada, T. Okano, Y. Sakurai, K. Kataoka, S. Inoue, Polymer micelles as novel drug carrier: adriamycin-conjugated poly(ethylene glycol)-poly(aspartic acid) block copolymer, J. Contr. Release 11 (1990) 269–278.

[18] M. Yokoyama, M. Miyauchi, N. Yamada, T. Okano, Y. Sakurai, K. Kataoka, S. Inoue, Characterization and anticancer activity of the micelle-forming polymeric anticancer drug adriamycin-conjugated poly(ethylene glycol)-poly(aspartic acid) block copolymer, Cancer Res. 50 (1990) 1693–1700.

[19] Y.I. Jeong, H.S. Na, K.O. Cho, H.C. Lee, J.W. Nah, C.S. Cho, Antitumor activity of adriamycin-incorporated polymeric micelles of poly([gamma]-benzyl l-glutamate)/poly(ethylene oxide), Int. J. Pharm. 365 (2009) 150–156.

[20] H.L. Wong, A.M. Rauth, R. Bendayan, X.Y. Wu, In vivo evaluation of a new polymer-lipid hybrid nanoparticle (PLN) formulation of doxorubicin in a murine solid tumor model, Eur. J. Pharm. Biopharm. 65 (2007) 300–308.

[21] R.K. Subedi, K.W. Kang, H.K. Choi, Preparation and characterization of solid lipid nanoparticles loaded with doxorubicin, Eur. J. Pharm. Sci. 37 (2009) 508–513.

[22] K. Kazunori, S.K. Glenn, Y. Masayuki, O. Teruo, S. Yasuhisa, Block copolymer micelles as vehicles for drug delivery, J. Contr. Release 24 (1993) 119–132.

[23] R. Gref, Y. Minamitake, M.T. Peracchia, V. Trubetskoy, V. Torchilin, R. Langer, Biodegradable long-circulating polymeric nanospheres, Science 263 (1994) 1600–1603.

[24] M. Yokoyama, T. Okano, Y. Sakurai, H. Ekimoto, C. Shibazaki, K. Kataoka, Toxicity and antitumor activity against solid tumors of micelle-forming

Author's personal copy

polymeric anticancer drug and its extremely long circulation in blood, Cancer Res. 51 (1991) 3229–3236.
[25] A. Miwa, A. Ishibe, M. Nakano, T. Yamahira, S. Itai, S. Jinno, H. Kawahara, Development of novel chitosan derivatives as micellar carriers of taxol, Pharm. Res. 15 (1998) 1844–1850.
[26] Y.I. Son, J.S. Jang, Y.W. Cho, H. Chung, R.W. Park, I.C. Kwon, I.S. Kim, J.Y. Park, S.B. Seo, C.R. Park, S.Y. Jeong, Biodistribution and anti-tumor efficacy of doxorubicin loaded glycol-chitosan nanoaggregates by EPR effect, J. Contr. Release 91 (2003) 135–145.
[27] H.S. Yoo, T.G. Park, Biodegradable polymeric micelles composed of doxorubicin conjugated PLGA–PEG block copolymer, J. Contr. Release 70 (2001) 63–70.
[28] D.C. Bibby, J.E. Talmadge, M.K. Dalal, S.G. Kurz, K.M. Chytil, S.E. Barry, D.G. Shand, M. Steiert, Pharmacokinetics and biodistribution of RGD-targeted doxorubicin-loaded nanoparticles in tumor-bearing mice, Int. J. Pharm. 293 (2005) 281–290.
[29] A.M. Al-Abd, N.H. Kim, S.C. Song, S.J. Lee, H.J. Kuh, A simple HPLC method for doxorubicin in plasma and tissues of nude mice, Arch. Pharm. Res. 32 (2009) 605–611.
[30] T.E. Mürdter, B. Sperker, K. Bosslet, P. Fritz, H.K. Kroemer, Simultaneous high-performance liquid chromatographic determination of a glucuronyl prodrug of doxorubicin, doxorubicin and its metabolites in human lung tissue, J. Chromatogr. B. Biomed. Sci. Appl. 709 (1998) 289–295.
[31] S.R. Urva, B.S. Shin, V.C. Yang, J.P. Balthasar, Sensitive high performance liquid chromatographic assay for assessment of doxorubicin pharmacokinetics in mouse plasma and tissues, J. Chromatogr. B. Anal. Technol. Biomed. Life Sci. 877 (2009) 837–841.
[32] R. Ricciarello, S. Pichini, R. Pacifici, I. Altieri, M. Pellegrini, A. Fattorossi, P. Zuccaro, Simultaneous determination of epirubicin, doxorubicin and their principal metabolites in human plasma by high-performance liquid chromatography and electrochemical detection, J. Chromatogr. B. Biomed. Sci. Appl. 707 (1998) 219–225.
[33] D. Kim, Z.G. Gao, E.S. Lee, Y.H. Bae, In vivo evaluation of doxorubicin-loaded polymeric micelles targeting folate receptors and early endosomal pH in drug-resistant ovarian cancer, Mol. Pharm. 6 (2009) 1353–1362.
[34] R.D. Arnold, J.E. Slack, R.M. Straubinger, Quantification of doxorubicin and metabolites in rat plasma and small volume tissue samples by liquid chromatography/electrospray tandem mass spectroscopy, J. Chromatogr. B. Anal. Technol. Biomed. Life Sci. 808 (2004) 141–152.
[35] H. Hasanzadeh, M. Mokhtari-Dizaji, S.Z. Bathaie, Z.M. Hassan, V. Nilchiani, H. Goudarzi, Enhancement and control of acoustic cavitation yield by low level dual frequency sonication: a subharmonic analysis, Ultrason. Sonochem. 18 (2011) 394–400.
[36] J.G. Shiah, Y. Sun, C.M. Peterson, J. Kopecek, Biodistribution of free and N-(2-hydroxypropyl) methacrylamide copolymer-bound mesochlorin e_6 and adriamycin in nude mice bearing human ovarian carcinoma OVCAR-3 xenografts, J. Contr. Release 61 (1999) 145–157.
[37] Q. Zhou, B. Chowbay, Determination of doxorubicin and its metabolites in rat serum and bile by LC: application to preclinical pharmacokinetic studies, J. Pharm. Biomed. Anal. 30 (2002) 1063–1074.